Appl. Phys. B 50, 345–354 (1990)

Applied Physics B Photophysics and Laser Chemistry

Efficient Optically Pumped NH_3 Amplifiers in the 10–12 μm Region

J. D. White, D. M. Bruce, P. H. Beckwith*, and J. Reid*

Department of Engineering Physics, McMaster University, Hamilton, Ontario L8S 4M1, Canada

Received 12 December 1989/Accepted 19 January 1990

Abstract. A pulsed transversely excited CO_2 laser operating on the $9R(30)$ transition is used to optically pump mixtures of NH_3 in buffer gas. A simple oscillator/amplifier system characterizes the performance of the NH_3 amplifier in the 11 μm region. Small-signal gain coefficients of $>10\%$/cm measured on the $aQ(3,3)$ transition at 10.7 μm, while pump conversion efficiencies of $\sim 50\%$ are shown to occur under saturation conditions. The NH_3 laser system is described by a rate-equation model, which is validated by comparison with experiment over a wide range of operating conditions. Measurements are made for NH_3 concentrations ranging from 0.05 to 0.2%, with Ar, N_2, and He buffer gas pressures from 170 to 700 Torr, and for gas temperatures from 200 to 300 K. Optically pumped NH_3 is shown to be a versatile and efficient system for the amplification of mid-infrared radiation.

PACS: 33.80.Be, 42.55.Hq, 42.60.By

Optically pumped NH_3 lasers have been widely investigated as sources of line-tunable radiation in the 10 to 13 μm region. Pulsed, transversely-excited (TE) CO_2 lasers are commonly used as the optical pump with the goal of developing efficient, line-tunable oscillators. There are now over 50 known NH_3 laser lines in the 10.3 to 13.8 μm region [1, 2], while measured pulse energies of 1.5 J [3] and conversion efficiencies of 28% [4] make NH_3 the most powerful and efficient optically pumped mid-infrared laser. The NH_3 laser has been used for isotope selective dissociation of CCl_4 [5], SeF_6 [6] and for tritium/deuterium separation [7]. However, only limited investigations have been carried out to characterize the behavior of optically pumped NH_3 as an amplifier [8–10].

In this paper, we report detailed measurements of the performance of NH_3 amplifiers under both small-signal and saturated gain conditions. The measured gain coefficients are compared with the predictions of a rate equation model developed by Morrison [9–12]. We have validated the model by comparison with experiment over a wide range of amplifier pressures (170–700 Torr), temperatures (200–300 K), mixtures (0.05–0.2% NH_3) and buffer gases (Ar, N_2, and He). The CO_2 pump intensities range from 20 to 120 kW/cm^2. Gain measurements were made for several different NH_3 transitions, and agreement with the model was better than $\pm 15\%$ under all conditions.

The main thrust of our experiments was to determine if optically pumped NH_3 can be used to replace TE CO_2 discharges as amplifier modules in laser-radar (LIDAR) systems. Optically pumped NH_3 has significant gain in the 10.8 μm region. We measured gain coefficients ranging from 5 to 10%/cm on the $aQ(3,3)$ transition at 930.76 cm^{-1}, and obtained a power conversion efficiency from the pump beam of 46%. This type of performance makes optically pumped NH_3 an attractive candidate for those LIDAR systems which require amplifier modules with large bandwidth, high gain, excellent optical quality, and the ability to amplify long pulses without excessive thermal distortion.

The next section explains the rate equation model used to describe the dynamics of the optically pumped NH_3 system. The experimental apparatus and results are described in Sects. 2–4, while a discussion and conclusions are presented in Sect. 5.

* Present address: Lumonics Inc., 105 Schneider Rd., Kanata, Ontario K2K 1Y3, Canada

1. Theory

Several different CO_2 transitions have been used to optically pump NH_3, but the most effective for line-tunable operation is the $9R(30)$ CO_2 transition at 1084.635 cm^{-1}. The linecenter of the $9R(30)$ CO_2 transition lies 184 MHz from the $sR(5,0)$ linecenter of NH_3, but is also in close coincidence to additional lines in the $sR(5,K)$ multiplet. The upper trace in Fig. 1 illustrates the spectral features in the 1084.6 cm^{-1} region. The pumping and collisional transfer processes relevant to laser operation are indicated schematically in the middle diagram, while the lower portion of Fig. 1 shows the relative gain coefficients for the stronger v_2 transitions under typical pumping conditions.

To produce line-tunable amplification in the mid-infrared, it is first necessary to transfer population from the ground level ($v_2=0$) to the $v_2=1$ vibrational level of NH_3. This transfer is accomplished by pumping the $sR(5,K)$ multiplet with resonant laser radiation. A mechanism is also required to distribute the population from the pumped rotational states in the upper vibrational level to the companion rotational states, and to repopulate the lower pumped state. This redistribution is achieved by diluting the NH_3 in a buffer gas such as Ar or N_2. Typically, NH_3 makes up less than 1% of the gas mixture, and collisions between

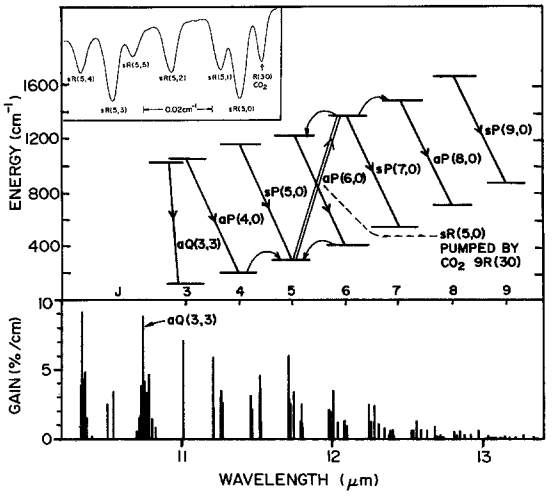

Fig. 1. Spectral features and energy levels of NH_3 relevant to laser operation. The upper trace is a tunable diode laser scan of NH_3 and CO_2 near 1084.6 cm^{-1}, showing the proximity of the CO_2 $9R(30)$ line to the $sR(5,0)$ and $sR(5,1)$ transitions in NH_3 (frequency offsets of 184 and 356 MHz, respectively). The middle section is an energy-level diagram of NH_3 showing several transitions that have gain when the $sR(5,0)$ transition is pumped. For simplicity mostly $K=0$ levels are shown. The curved arrows represent the collisional processes that thermalize the population in the upper and lower levels. The lowest portion of the figure shows a gain spectrum attained under typical pumping conditions

the NH_3 and the buffer gas produce rapid rotational relaxation in both upper and lower vibrational levels. By pumping on an R-branch transition, inversion can potentially be created on all Q and P-branch transitions [13]. As both the pump and lasing transitions occur in the strong, fundamental v_2 vibrational mode of NH_3, very efficient operation is expected [14].

We have developed a rate-equation model to describe the dynamics of population inversion in optically pumped NH_3 lasers. The model evaluates changes in populations based on two main assumptions: (1) the rotational populations are always thermalized, except for the levels of the pumped transition, and (2) the ortho-species of NH_3 (angular momentum quantum number $K=3n$), and the para-species ($K=3n\pm1$) can be treated as two independent species. Assumption (1) is justified as the rotational relaxation rate in dilute NH_3 mixtures is much faster than the vibrational-translational (V–T) relaxation rate [11], and the population distribution remains close to thermal equilibrium in those levels not directly coupled to the pump radiation. Assumption (2) has been shown to be a very good approximation in experiments in which only a single species of NH_3 was optically pumped [1, 11], and recent direct measurements of collisional relaxation rates have shown that the rate of vibrational energy transfer between ortho- and para-NH_3 is very slow [15].

A computer model has been used successfully to calculate the gain in both cw and pulsed NH_3 systems [9–12]. As the pump and probe pulses employed in the present series of experiments have a much longer time duration than the characteristic V–T relaxation time of the NH_3 gas mixtures, one can treat the laser system in a quasi-cw fashion. We therefore follow the cw treatment described in detail in Ref. [11], with a few minor modifications to account for the much higher gas pressures used in the present work, and to include the results of more recent measurements of relaxation rates in NH_3. In the model the total NH_3 population is assumed to lie in the ground, first, and second excited states of the v_2 mode.

These vibrational levels are treated as harmonic with a fundamental frequency $\nu=950$ cm^{-1}, but the inversion splitting of 36 cm^{-1} in the $v_2=1$ state is treated explicitly to ensure that saturation of the $sR(5,0)$ transition is calculated accurately. All the pump and emission transitions of interest in this paper occur between the $v_2=0$ and $v_2=1$ levels. Thus the equations are written chiefly in terms of N_0 and N_1, the populations of the two lower vibrational levels. The total population N is the sum of N_0, N_1, and N_2, where N_2 is the population of the second excited state. The complete rate equations for N_0 and N_1 and the two

rotational levels of the pumped transitions are:

$$\frac{dN_0}{dt} = \frac{(N_1 - x_v N_0)}{\tau_{VT}} + \frac{2(N_1^2 - N_0 N_2)}{N \cdot \tau_{VV}} - W_p \Delta r$$
$$\equiv P_0 - W_p \Delta r \quad (1)$$

$$\frac{dN_1}{dt} = \frac{[2N_2 - (1+2x_v)N_1 + x_v N_0]}{\tau_{VT}} - \frac{4(N_1^2 - N_0 N_2)}{N \cdot \tau_{VV}}$$
$$+ W_p \Delta r \equiv$$
$$\equiv -P_1 + W_p \Delta r \quad (2)$$

$$\frac{dr_0}{dt} = \frac{-(r_0 - r_0^e)}{\tau_0} - W_p \Delta r + P_0 \left(\frac{r_0}{N_0}\right) \quad (3)$$

$$\frac{dr_1}{dt} = \frac{-(r_1 - r_1^e)}{\tau_1} + W_p \Delta r - P_1 \left(\frac{r_1}{N_1}\right) \quad (4)$$

and

$$N = N_0 + N_1 + N_2$$
$$x_v = \exp\left(\frac{-h\nu}{k_B T}\right).$$

The pumping rate from rotational level r_0 in N_0 to rotational level r_1 in N_1 is

$$W_p \Delta r = \left(\frac{I_p}{h\nu_p}\right) \sigma \left[r_0 - r_1 \left(\frac{g_0}{g_1}\right)\right], \quad (5)$$

where I_p is the pump intensity at the frequency ν_p, σ is the absorption cross section, and g_0 and g_1 are the degeneracies of r_0 and r_1. The absorption cross section is calculated under the assumption that all the $9R(30)$ pump radiation is centred at a 184 MHz frequency offset from the $sR(5,0)$ transition. At thermal equilibrium, with no pump present, $r_i^e = f_i N_i$. With the presence of the pump (r_i is counted in N_i),

$$r_i^e = f_i \frac{(N_i - r_i)}{(1 - f_i)}. \quad (6)$$

Throughout this paper r_0 is the $s(5,0)$ level in the ground state, while r_1 is the $a(6,0)$ level in the $v_2 = 1$ vibrational state.

The values of the relaxation rates in the model are obtained in the following manner. The VT relaxation rate τ_{VT}^{-1} is given by [15, 16]

$$\tau_{VT}^{-1} = (k_{NH_3} p_{NH_3} + k_m p_m), \quad (7)$$

where the k's are rates and the p's are pressures of NH_3 and a buffer gas m. The values of k_{NH_3} and k_{N_2} are taken from [15], while k_{Ar} and k_{He} are taken from the work of Hovis and Moore [16]. Recent experimental work has shown that the vibrational-vibrational rate, τ_{VV}^{-1}, is insignificant under typical NH_3 laser conditions, and that the population N_2 is simply given by [17]:

$$N_2 = N_1 x_v. \quad (8)$$

Thus N_2 is always $\leqq 1\%$ of N_1 for gas temperatures in the range 200–300 K. Within the accuracy of the present model, the population in N_2 can be ignored, and we achieve the same result in the computer simulation by making τ_{VV} very long compared with all other relaxation rates. In previous work we have assumed that the rotational rates τ_0^{-1} and τ_1^{-1} are defined by the pressure-broadened halfwidth at half-maximum of the absorption line $\Delta\nu$ given by [11]:

$$\Delta\nu = \left(\frac{\Delta\nu}{p}\right)_{NH_3} p_{NH_3} + \left(\frac{\Delta\nu}{p}\right)_m p_m, \quad (9)$$
$$= \frac{1}{4\pi}\left(\frac{1}{\tau_0} + \frac{1}{\tau_1}\right).$$

This formula gives reasonable agreement with experimental measurements of small-signal gain, although there is some uncertainty in the value of the ratio $y = \tau_0/\tau_1$. However, as described in Sect. 4, measurements of saturated gain coefficients demonstrate that (9) overestimates the rate of rotational population transfer. We therefore introduce a variable parameter, K, such that

$$K\Delta\nu = \frac{1}{4\pi}\left(\frac{1}{\tau_0} + \frac{1}{\tau_1}\right), \quad (10)$$

where $K < 1$, and is adjusted to give a best-fit to the experimental results.

For the case of quasi-cw pumping, when the pump intensity I_p varies slowly on the timescale of τ_{VT}, the rate equations are solved for the final populations by setting all the time derivatives equal to zero. The solution is not analytic because the equations are nonlinear. Hence a numerical root-finding computer program is employed to solve for N_0, N_1, and N_2. The final step in the model is the evaluation of the gain spectrum from the vibrational populations under the assumption of rotational thermalization. Rather than use the values of N_1 and N_0 directly, we define two parameters that express the degree of vibrational inversion, N_1/N_0, and the fractional population in the ground and $v_2 = 1$ states, $(N_0 + N_1)/N$. The value of N_1/N_0 specifies the gain distribution, whereas $(N_0 + N_1)/N$ gives the fraction of the total NH_3 molecules which remain in the upper and lower laser levels. (As V–V transfer into the $v_2 = 2$ level is slow [17], $(N_0 + N_1)/N$ is typically $\geqq 0.99$). A separate subroutine takes specific values of these two parameters together with the NH_3 partial pressure, the total pressure broadening due to the buffer gas, and the rotational temperature to evaluate the gain on the NH_3 transitions of interest. This gain calculation includes the effect of the inversion splitting of all the vibrational states into symmetric (s) and antisymmetric (a) levels. The splitting is negligible in the

ground state (0.8 cm^{-1}). However, in the $v_2=1$ state the splitting is 36 cm^{-1}, and this leads to the prediction of significantly higher gain coefficients for the a-transitions than for the corresponding s-transitions.

In many of the experiments described in this paper, the intensities of both the pump and probe beams vary significantly along the length of the amplifier. Thus a "point model" which deals with fixed intensities is not appropriate. The computer model is designed to treat an amplifier cell as many short sections, and to automatically handle the changes in intensity as the beams propagate. While the ortho and para species of NH_3 are treated separately in the calculation, pump depletion due to absorption by *all* the transitions in the $sR(5, K)$ multiplet is taken into account.

2. Experimental Apparatus and Measurement Technique

Figure 2 is a schematic diagram of the apparatus. A simple oscillator/amplifier configuration is used to measure gain coefficients in the optically-pumped medium. A single TE CO_2 laser pumps both the oscillator and the amplifier. The TE laser is a Lumonics K-902 with a discharge volume of $88 \times 3.5 \times 3.3$ cm^3. The laser is operated at ~ 85 Torr with a 8% CO_2 : 13% N_2 : 79% He mixture. This low pressure ensures that the frequency bandwidth of the CO_2 radiation is relatively narrow, and that the pulsed output has a long duration suitable for Doppler-LIDAR systems. When tuned to the $9R(30)$ transition, the laser gives an output pulse ~ 40 μs long with a total energy of 2.5 J.

The CO_2 laser pulse is split into two beams; 36% of the pulse pumps the oscillator, while the remaining pulse energy is directed into the amplifier. The NH_3 oscillator contains a 1-m long pyrex tube sealed with KCl Brewster windows and cooled with dry ice. Typically, the pyrex tube is filled with 0.05% NH_3 in Ar at a total pressure of 50 to 140 Torr. This tube operates sealed-off, and one gas mixture lasts for many months. The NH_3 laser cavity is formed by a 60% reflecting mirror and a 135 lines/mm grating. For the gain saturation measurements, the conditions in the NH_3 oscillator were carefully optimised to produce $aQ(3, 3)$ NH_3 pulses with high energy and maximum peak power.

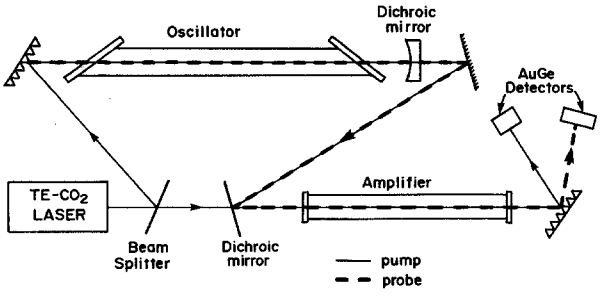

Fig. 2. Schematic diagram of the apparatus for measuring gain in optically pumped NH_3

The probe from the oscillator and the second 9 μm pump beam are combined at a dichroic mirror before passing through the amplifier. Care was taken to optimise the transmission of both pump and probe pulses through the system. Typically, 0.8 J of pump radiation and 75 mJ of $aQ(3, 3)$ probe radiation are incident upon the entrance window of the amplifier. When the amplifier cell is empty, these pulses result in peak powers of ~ 110 kW/cm^2 (pump) and ~ 15 kW/cm^2 (probe) exiting the cell. For the small-signal gain measurements, the NH_3 oscillator was operated at lower pressures, and a series of attenuators were used to ensure that the peak pulse power of the probe was $\ll 1$ kW/cm^2. Two amplifier tubes were used in the present study; one was 60 cm long while the other was 120 cm long. Each tube was sealed with AR-coated ZnSe windows, could be cooled with dry ice, and was generally operated with a slowly flowing gas mixture. The 6.8 mm diameter tubes act as waveguides for both the pump and probe beams. The waveguide ensures that the pump beam is confined over the length of the cell, and that the pump and probe beams have a good spatial overlap. A second grating separates the pump and probe beam after passage through the amplifier; each pulse is detected by separate Au–Ge detectors. The detector signals are then recorded on a Tektronix 468 digital oscilloscope.

Measurement Technique

Figure 3 displays the three pulse shapes recorded by the oscilloscope during the measurements of small-signal gain. The probe pulses are recorded both with and without NH_3 gas in the 60 cm amplifier, and under small-signal gain conditions we measure peak amplifications in the range of 50 to 100 per pass. During the period of this study, both the pump and probe pulses were stable and reproducible. Typically, the peak powers varied by $\pm 3\%$ from shot-to-shot, and long term drifts during the course of an experiment were less than $\pm 5\%$. The lasers were generally operated at a repetition rate of 1 Hz, and in all cases 8 successive pulses were averaged by the oscilloscope before the data was transferred to a computer. The computer was used to calculate gain coefficients as a function of pump intensity, and to compare experiments with the predictions of the model.

To make accurate comparisons with the rate equation model, it is important that experimental parameters such as intensity and gas mixture be

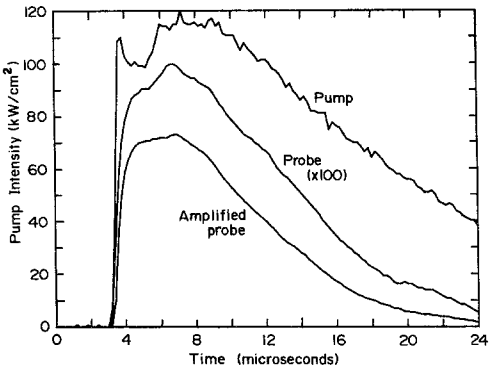

Fig. 3. Typical pulse shapes as recorded by the digital oscilloscope. In each case, eight successive pulses are averaged to produce the plots. The $9R(30)$ CO_2 pulse pumps a mixture of 0.1% NH_3 in Ar at a total pressure of 170 Torr and a temperature of 200 K. The $aQ(3,3)$ probe pulse is amplified by a factor of ~60 in the 60 cm amplifier tube

accurately known. We measure intensity by determining the energy of the laser pulses exiting the waveguide with a Gen-Tec ED-500 Joule meter, and scaling to the integrated area of the pulse as determined by the computer. We then divide by the area of the waveguide to determine the *average* intensity across the bore of the amplifier. In an empty waveguide, the pump and probe attenuation is small (< 10%/pass), and does not affect the model comparisons. However, there is a significant variation in the radial intensity distribution across the circular bore of amplifier. For both the pump and the probe, the measured intensity distribution corresponds closely to an EH_{11} waveguide mode. This radial intensity distribution is ignored in the model calculations, as discussed in Sects. 3 and 4.

If a reliable comparison is to be made between theory and experiment, it is essential that the concentration of the gas mixture be accurately known. As NH_3 is a reactive gas, and tends to be both absorbed and desorbed from the walls of a cell, some care must be taken in determining the gas concentration. We have used a variety of techniques for ensuring that the NH_3 concentration present within the amplifier cell is known to $\pm 10\%$. The measurements presented in this paper were all made with gas mixtures flowing slowly through the amplifier tube. A gas cylinder containing ~1% NH_3 in Ar was purchased from Canadian Liquid Air. The manufacturer's measured concentration was 0.745% NH_3 in Ar. We made an independent check on the cylinder concentration using an infrared absorption cell and a 12 μm tunable diode laser [18]. Our measured concentration was 0.75% $\pm 0.03\%$. The gas from the cylinder was further diluted with Ar using calibrated flowmeters. We estimate that the resultant gas concentration was accurate to better than $\pm 10\%$. A final check on gas concentration was made by measuring the probe absorption in a 10 cm, flowing gas cell. The gas flowing through the cell was identical to that flowing through the amplifier. It is an easy matter to convert the small-signal absorption, as measured on the $aQ(3,3)$ transition, into an NH_3 concentration [18]. In all cases, the measured absorption on $aQ(3,3)$ agreed with that predicted from the flowmeter settings to better than $\pm 10\%$.

3. Results of Small-Signal Gain Measurements

The 60-cm amplifier cell was used for the small-signal gain measurements. Care was taken to ensure that the detector response was linear, and that measurements were made in the small-signal regime. Figure 4 is typical of the data obtained from the small-signal gain measurements. The experimental results are evaluated by calculating gain coefficients as a function of time, and then plotting the gain coefficient as a function of the pump intensity at that time. In this fashion, the three pulses shown in Fig. 3 can be converted into a complete record of gain coefficient versus pump intensity. As a check on experimental consistency, we attenuated the pump pulse by known factors to record the data of Fig. 4. Note that the measured gain coefficient at 30 kW/cm² pump intensity, for example, is relatively insensitive to whether it is measured near the peak of a weak pump pulse or in the tail of the unattenuated pump pulse. This type of measurement also confirms that gas heating has little effect on the gain coefficients at 170 Torr.

From Fig. 4, it can be seen that the experimental and calculated gain coefficients are insensitive to pump intensity at high intensities. The high pump intensity strongly saturates the absorption on the $sR(5,0)$ transition, and the population inversion on $aQ(3,3)$ is

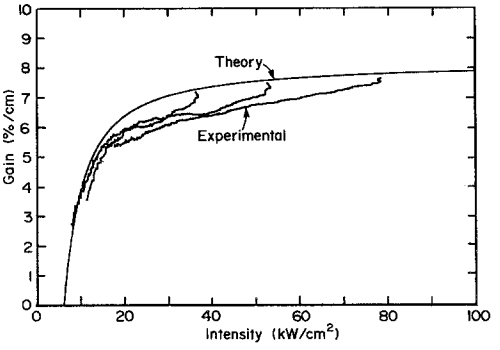

Fig. 4. Measured and calculated small-signal gain coefficients on the $aQ(3,3)$ transition as a function of pump intensity for a 0.094% NH_3 in Ar mixture at 170 Torr and 200 K. The pump pulse was progressively attenuated (×0.68 and ×0.47) to produce the three experimental traces. The calculations are performed with the rotational coupling parameter, K, set equal to 0.55 (see text)

Table 1. Comparison of results obtained for a nominal 0.1% NH_3 in Ar mixture at 170 Torr and 200 K. Pump intensity is ~ 75 kW/cm^2

Date of measurement	Measured gain coefficient on $aQ(3,3)$ [%/cm]	Measured absorption coefficient in 10 cm room temperature cell [%/cm]	Ratio[a]
June 20th	6.6	9.5	0.70
June 19th	6.7	9.7	0.69
June 18th	5.7	7.0	0.81
June 12th	6.1	9.0	0.68
June 11th	7.8	12.0	0.65
May 20th	6.1	8.8	0.70

[a] Theory predicts a ratio of 0.83 ($K=1$) and 0.79 ($K=0.55$)

Table 2. Results of small-signal gain measurements made over a wide range of conditions

Conditions of measurements	Gain coefficient [%/cm]	
	Expt	Theory ($K=0.55$)
Probe operating on $sP(3,0)$, 0.11% NH_3 in Ar at 170 Torr and 200 K; 80 kW/cm^2 pump	4.7 ± 0.3	5.0–5.2[a]
As above, but 360 Torr	4.2 ± 0.3	4.5–5.2[a]
Probe operating on $aQ(3,3)$, 0.23% NH_3 in N_2 at 55 Torr and 200 K; 80 kW/cm^2 pump	6.6	7.6
As above, but 140 Torr and 75 kW/cm^2 pump	5.9	6.5
0.058% NH_3 in He at 280 Torr and 200 K; 75 kW/cm^2 pump	5.8	5.8
0.054% NH_3 in Ar at 480 Torr and 200 K; 75 kW/cm^2 pump	3.6	3.7
0.053% NH_3 in Ar at 170 Torr and 200 K; 80 kW/cm^2 pump	4.0	4.1
0.093% NH_3 in Ar at 170 Torr and 300 K, 80 kW/cm^2 pump	2.5	2.8
0.095% NH_3 in Ar at 360 Torr and 300 K, 80 kW/cm^2 pump	2.1	2.4

[a] Exact value of gain depends upon degree of overlap with nearby $sP(3,1)$

no longer dependent upon the exact value of the pump intensity, provided saturation is maintained. Under these conditions, the measured gain coefficients are independent of the exact pump distribution in the amplifier cell, both longitudinally and radially. Hence, this situation is an ideal one for a careful comparison of theory and experiment. We have treated the 170 Torr, 0.1% NH_3 mixture at 200 K as a standard, and have measured gain coefficients many times over a one month period. In each case, the probe absorption was also measured in the 10 cm room temperature cell to determine the exact gas mixture. Results are summarized in Table 1. The important parameter in this table is the ratio of gain/absorption, as this factor is independent of minor variations of gas concentration. The reproducibility of this factor indicates the overall reproducibility of the experiment.

In Fig. 4 and Table 1, the experimental results are compared with two different calculations using $K=1$, and $K=0.55$. If K is set equal to 1.0, then the model assumes that all pressure-broadening collisions which contribute to the linewidth also transfer rotational population from the pumped to the unpumped levels, i.e., τ_0 and τ_1 have the minimum possible value. Consequently, collisional transfer from the upper pumped level, $a(6,0)$ of $v_2=1$, is most effective, and the gain on $aQ(3,3)$ is maximized. In the next section we show that $K=0.55$ gives the best fit to the gain saturation data, and with this value in the model, small-signal gain is reduced by approximately 5%. The experimental measurements of small-signal gain are not accurate enough to distinguish between the two values of K, but the overall agreement between experiment and calculation is satisfactory.

We have compared theory and experiment over a wide range of amplifier conditions. Figure 5 shows results obtained at 360 Torr, while Table 2 lists results obtained for ~ 80 kW/cm^2 pump intensity. Note that Table 2 includes measurements made with a second probe transition, with He as a buffer gas, and at both 200 K and at room temperature. The good agreement demonstrated in Table 2 between theory and experi-

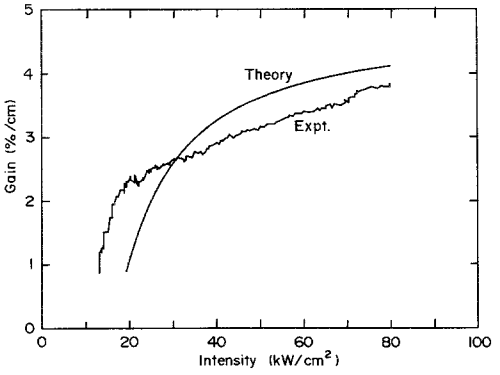

Fig. 5. Repeat of Fig. 4 for a 0.053% NH_3 in Ar mixture at 360 Torr and 200 K. Data is recorded for the full-intensity pump pulse only

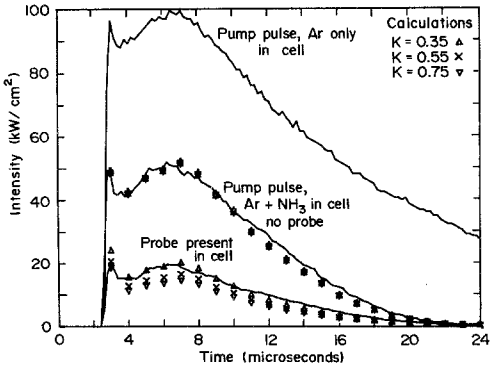

Fig. 7. Attenuation of the $9R(30)$ pump pulse under the conditions given in Fig. 6. Theoretical points are calculated with $K=0.35$, 0.55, and 0.75

ment gives us confidence that the model can be reliably used to calculate small-signal gain coefficients over a wide range of amplifier conditions.

4. Results of Gain Saturation Measurements

The small-signal gain measurements described in the previous section were encouraging–large gain coefficients can be created by optical pumping, and the model enables accurate predictions to be made for a wide range of operating conditions. However, in many practical applications the NH_3 amplifiers will operate not in the small-signal regime, but in the saturated regime. The measurements described in this section were designed to evaluate amplifier performance when the probe laser power was increased to ~ 10 kW/cm^2.

The majority of the saturation measurements were made on an amplifier cell which was 120 cm long. This length allowed efficient conversion of the $9R(30)$ pump beam into $aQ(3,3)$ probe radiation. Figures 6 and 7 are typical of the data recorded in the 120 cm cell. The sectioned-cell model can be used to predict the amplifier performance for the conditions of Figs. 6 and 7. The model predictions, calculated by splitting the amplifier into 800 sections, are given for three values of K. Note that the calculated attenuation of the pump pulse in the absence of the probe beam does not vary with K [19]. Hence the good agreement between theory and experiment confirms that the NH_3 concentration is correct. In a sense, a measurement of pump transmission in the absence of the probe beam is equivalent to an in situ measurement of NH_3 concentration.

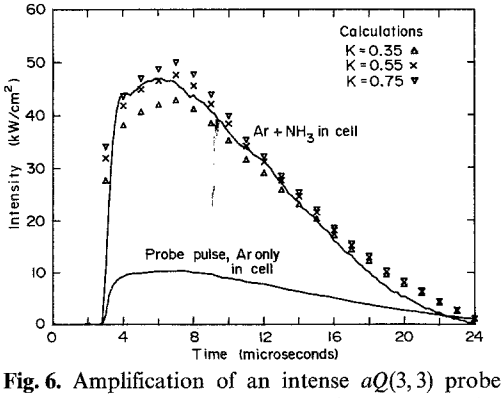

Fig. 6. Amplification of an intense $aQ(3,3)$ probe pulse in a 120 cm amplifier cell. Gas mixture is 0.09% NH_3 in 360 Torr Ar at 200 K. The theoretical points are calculated with $K=0.35$, 0.55, and 0.75

When a strong probe beam is present in the amplifier, several equations must be added to the model to account for gain saturation. These equations,

$$\frac{ds_0}{dt} = \frac{-(s_0 - s_0^e)}{\tau_0} - W_s \Delta s + P_0\left(\frac{s_0}{N_0}\right) \tag{10}$$

$$\frac{ds_1}{dt} = \frac{-(s_1 - s_1^e)}{\tau_1} + W_s \Delta s - P_1\left(\frac{s_1}{N_1}\right), \tag{11}$$

account for the change in the populations of the lower, s_0, and upper, s_1, probed levels due to the stimulated emission term:

$$W_s \Delta s = \left(\frac{I_s}{h\nu_s}\right)\sigma_s\left[s_0 - s_1\frac{g_{s0}}{s_{s1}}\right]. \tag{12}$$

I_s is the probe intensity at the frequency ν_s, and the other terms are defined as in (5).

When the set of equations (1) through (12) are solved for quasi-cw intensities, the behaviour of the amplifier under saturation conditions is found to depend somewhat upon the value of K. For example, the efficiency with which the $aQ(3,3)$ probe can convert photons from the $9R(30)$ pump depends strongly upon the rate of transfer of population from the $a(6,0)$ level to the $s(3,3)$ level in the $v_2=1$ vibrational level in NH_3. Figures 6 and 7 clearly indicate the reduction in conversion efficiency as K is changed from 0.75 to 0.35.

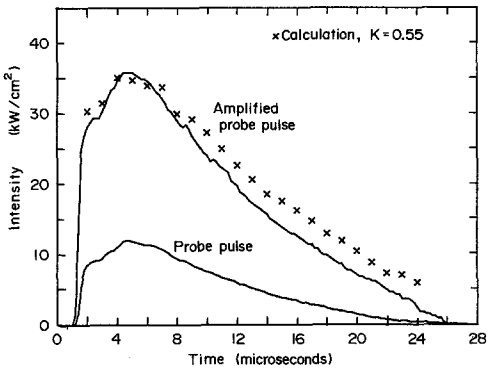

Fig. 8. Repeat of Fig. 6 for a 120 cm amplifier cell operating at 200 K and 170 Torr. The gas mixture is 0.1% NH_3 in Ar. Theoretical points are calculated with $K=0.55$

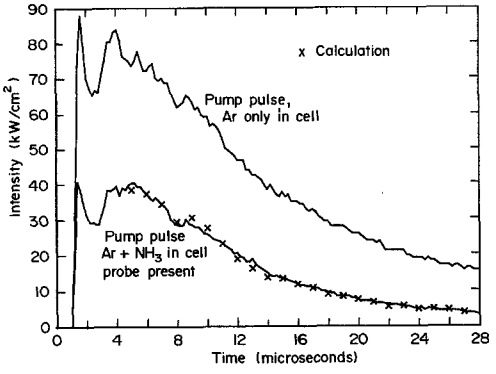

Fig. 9. Attenuation of the 9*R*(30) pump pulse under the conditions given in Fig. 8. Theoretical points are calculated with $K=0.55$

We have repeated the type of measurements shown in Figs. 6 and 7 for a range of operating conditions, and used K as a variable to obtain the best fit between theory and experiment. In general, we find that all our experimental results can be modelled with values of K ranging from 0.35 to 0.75. We interpret the apparent variation in K as resulting from minor experimental irreproducibilities. When all our experimental results are taken into consideration, as made over a wide range of mixtures, pressures and temperatures, the optimum value of K appears to be 0.55. Hence, all calculations made in the rest of this paper are carried out with $K=0.55$. Figures 8 and 9 compare theory and experiment for a 120 cm amplifier cell operating at 170 Torr. Once again there is good agreement as a function of time, confirming that the model is valid for a wide range of pump and probe intensities. We have obtained similar agreement for NH_3 concentrations ranging from 0.05% to 0.2% NH_3, gas temperatures ranging from 200 to 300 K, and for amplifier lengths of 60 and 120 cm. The measurements described in this section and the previous section give us confidence that the rate equation model can accurately predict amplifier performance throughout the parameter range of interest in the present study. Model predictions are discussed in the next section.

5. Discussion and Conclusions

The phenomenological constant, K, was introduced into the model to account for the experimental gain saturation results. The optimum value of $K=0.55$ indicates that the transfer of energy between specific rotational energy levels may not proceed as fast as the collisional broadening rate. K may also account for the radial variation of the pump and probe intensities. All calculations are simply carried out using *average* intensities. In any event, the model with $K=0.55$ gives good agreement with experiment.

Efficiencies

Section 3 illustrates that large values of small-signal gain can easily be obtained in optically pumped NH_3, while Sect. 4 shows that efficient energy extraction can also be achieved. Note that in Fig. 6, the peak probe intensity is amplified from 10 kW/cm^2 to 47 kW/cm^2, an increase of 37 kW/cm^2. Simultaneously, the pump intensity is reduced from 100 kW/cm^2 to 20 kW/cm^2, a reduction of 80 kW/cm^2. Thus the measured conversion efficiency is 46%. A probe intensity increase of 37 kW/cm^2 is equivalent to a power extraction of approximately 370 kW/l from the amplifier volume. For pulse lengths $\geqq 30$ μs, energy extractions >10 J/l can be attained, a significant increase over the 0.5 J/l reported by Deka et al. [20]. An alternative way of viewing the results shown in Figs. 6 and 7 is to calculate the number of NH_3 molecules which take part in the conversion of pump to probe radiation, if one assumes a single NH_3 molecule is required to produce one additional probe photon. At a 300 kW/l conversion rate, every NH_3 molecule in the gas (both ortho and para species) contributes once per microsecond, i.e., during the pulses shown in Figs. 6 and 7 approximately 10 probe photons are generated for every NH_3 molecule in the gas.

For optimum amplifier conditions, the model predicts overall power conversion efficiencies of 50% for operation at 200 K, and as high as 55% if the amplifier is cooled to 150 K (at room temperature, efficiency is reduced to 35%). Most of the pump radiation which is not converted into $aQ(3,3)$ photons is used to maintain the population inversion against V–T collisions [21], while a few percent of the pump photons exit the amplifier, even under optimum conditions. As window and waveguide losses are negligible in a well-designed amplifier, experimental power efficiencies of 50% (equivalent to photon conversion efficiencies of $\sim 60\%$) should be achievable.

The optical pump for the NH_3 amplifier can be a multimode CO_2 pulse produced by a low or high pressure discharge, while the amplified $aQ(3,3)$ signal can be a single-mode Gaussian beam with a frequency bandwidth limited only by the pressure in the NH_3 amplifier. Hence, one can decouple the stringent optical requirements of a LIDAR pulse from the constraints imposed by the stability of a CO_2 discharge. The pump laser can operate with poor mode quality, while the waveguide NH_3 amplifier will provide good mode quality and the correct bandwidth by conversion to $aQ(3,3)$ radiation.

Heating Effects

The pump photons which are absorbed in the NH_3 gas eventually lead to gas heating. As the model gives an accurate representation of pump absorption (Fig. 7), it can be used to calculate gas heating. For dilute mixtures of NH_3, gas heating is proportional to the NH_3 concentration, and to the square of the total gas pressure. For a typical gas mixture of 0.1% NH_3 in 360 Torr Ar at 200 K, the rate of gas heating is ~ 1.5 K/μs. Thus pulses of 20 to 30 μs in length can be amplified before thermal effects become significant. If longer pulses are employed and gas heating is a concern, then larger amplifier cells (several metres) containing very dilute NH_3 ($\sim 0.01\%$) can be utilized. The optical pumping technique also allows a single pump laser to be split into several beams to pump a series of different waveguide amplifiers. These amplifiers can be separately optimised for amplification of weak pulses (pre-amp), as power amplifiers or as wide bandwidth amplifiers (high pressure).

Line-Tunability

Most of the experimental work in this paper was carried out on the $aQ(3,3)$ transition at 10.74 μm. A few measurements were made with the $sP(3,0)$ transition at 11.01 μm. However, gain exists on many other ortho and para transitions in the v_2 band of NH_3. Reference [1] lists 65 transitions in NH_3 covering the wavelength region from 10.3 to 13.8 μm. Table 3 lists a few of the stronger transitions, and indicates typical amplifier performance for each transition. Clearly, the $aQ(3,3)$ transition is one of the better transitions, but a similar performance can be obtained at several other wavelengths in the 11–12 μm region.

Oscillator Performance

This paper has only dealt with the performance of optically-pumped NH_3 as an amplifier. The rate equation model can also be used to predict the performance of a line-tunable NH_3 laser, and efficiencies similar to those shown in Table 3 can easily be attained. We have used the rate-equation model to predict the optimum operating conditions for an NH_3 laser, and have recently obtained multi-Joule output pulses in the 12 μm region, with conversion efficiencies of >40% [22]. To the best of our knowledge, these results represent both the maximum reported pulse energy and highest energy efficiency of any mid-

Table 3. Predicted performance of an NH_3 amplifier as a function of transition. Calculations are carried out for a 2 m amplifier containing 0.1% NH_3 in 170 Torr Ar at 200 K. It is assumed that the amplifier cell has negligible window and waveguide losses, and that the input intensities of the pump and probe are 100 kW/cm^2, and 10 kW/cm^2 respectively (Figs. 6 and 7)

Transition	Wavenumber	Small-signal gain Coefficient [%/cm]	Power conversion efficiency	
			Total[a] %	Effective[b] %
$aQ(3,3)$	930.75697	8.4	46.4	64.6
$aQ(6,6)$	927.32300	4.5	38.7	60.7
$sQ(3,3)$	967.34631	5.3	33.4	59.2
$aP(4,0)$	853.81790	5.8	54.9	63.9
$aP(4,3)$	851.32685	3.3	51.2	62.5
$aP(7,3)$	796.13417	1.3	26.4	47.9
$aP(8,3)$	778.29002	0.55	10.9	30.6
$aP(9,3)$	760.69388	0.20	3.6	13.7
$sP(3,0)$	908.19912	4.7	45.7	63.2
$sP(5,3)$	867.71961	2.5	42.8	60.0
$sP(6,3)$	847.57811	1.8	34.7	55.1
$sP(7,3)$	827.48779	1.0	20.4	43.9
$sP(8,3)$	807.47174	0.44	8.4	26.4

[a] Defined as (Probe out − Probe in)/(Pump in)
[b] Defined as (Probe out − Probe in)/(Pump in − Pump out)

infrared optically pumped laser. Further details on oscillator performance will be published separately.

Acknowledgement. We are grateful to Dr. H. Morrison of Ontario Hydro for many helpful discussions. This work was supported, in part, by Rockwell International Inc. and the Natural Science and Engineering Council of Canada.

References

1. D.F. Kroeker, J. Reid: Appl. Opt. **25**, 2929–2933 (1986)
2. *Handbook of Laser Science and Technology, Vol. II: Gas Lasers*, ed. by M.J. Weber (CRC, Florida 1982)
3. B.I. Vasil'ev, A.Z. Grasyuk, A.P. Dyad'kin, A.N. Sukhanov, A.B. Yastrebkov: Sov. J. Quantum Electron. **10**, 64–68 (1980) [Kvantovaya Elektron. **7**, 116–122 (1980)]
4. P.K. Gupta, A.K. Kar, M.R. Taghizadeh, R.G. Harrison: Appl. Phys. Lett. **39**, 32–34 (1981)
5. R.V. Ambartsumian, A.Z. Grasiuk, A.P. Pyadkin, N.P. Furzikov, V.S. Letokhov, B.I. Vasil'ev: Appl. Phys. **15**, 27–30 (1978)
6. J.J. Tiee, C. Wittig: Appl. Phys. Lett. **32**, 236–238 (1978)
7. F. Magnotta, I.P. Herman: J. Chem. Phys. **81**, 2363–2374 (1984)
8. H. Tashiro, T. Koizumi, K. Toyoda, S. Namba: Opt. Lett. **9**, 279–281 (1984)
9. H.D. Morrison, B.K. Garside, J. Reid: J. Opt. Soc. Am. B **2**, 535–540 (1985)
10. H.D. Morrison, B.K. Garside, J. Reid: IEEE J. QE-**20**, 1051–1060 (1984)
11. R.L. Sinclair, J. Reid, H.D. Morrison, B.K. Garside, C. Rolland: J. Opt. Soc. Am. B **2**, 800–806 (1985)
12. H.D. Morrison: "*Dynamics of Optically-Pumped Pulsed Mid-Infrared NH3 Lasers*", Ph. D. Thesis, McMaster University, 1985
13. A.L. Golger, V.S. Letokhov: Sov. J. Quantum Electron. **3**, 15–20 (1973) [Kvantovaya Elektron. **1**, 30–40 (1973)]
14. P.K. Gupta, S.C. Mehendale: Hyperfine Interactions **37**, 243–274 (1987)
15. D.J. Danagher, J. Reid: J. Chem. Phys. **86**, 5449–5455 (1987)
16. F.E. Hovis, C.B. Moore: J. Chem. Phys. **69**, 4947–4950 (1978); **72**, 2397–2402 (1980)
17. P. Dubé, J. Reid: J. Chem. Phys. **90**, 2892–2898 (1989)
18. P.H. Beckwith, D.J. Danagher, J. Reid: J. Mol. Spectrosc. **121**, 209–217 (1987)
19. In the absence of the probe field, the pump radiation must only maintain the $v_2=1$ vibrational population against collisional relaxation via V–T transfer. As the total population in the $v_2=1$ level is insensitive to the details of rotational transfer within the level, the pump absorption does not depend upon K
20. B.K. Deka, P.E. Dyer, I.K. Perera: Opt. Commun. **32**, 295–300 (1980)
21. In dilute mixtures of Ar, the NH_3 V–T rate varies from 6090 $Torr^{-1}\,s^{-1}$ at 300 K to 2393 $Torr^{-1}\,s^{-1}$ at 155 K [16]. This variation accounts for much of the reduction in efficiency as the amplifier is heated
22. D.M. Bruce, A. Chakrabarti, J. Reid, J.D. White: "Efficient, optically-pumped NH_3 oscillators and amplifiers operating in the mid-infrared", paper presented at the 1988 CLEO Conference, Anaheim, 1988